Stellar Evolution onto and off the Main Sequence

Stellar Structure

$$\frac{dP}{dM_r} = -\frac{GM_r}{4\pi r^4}$$

$$\frac{dr}{dM_r} = \frac{1}{4\pi r^2 \rho}$$

$$\frac{dT}{dM_r} = \begin{cases} -\frac{3\kappa}{64\pi^2 ac}\left(\frac{1}{T^3}\right)\left(\frac{L_r}{r^4}\right), & \nabla_{rad} < \nabla_{ad} \\ -\frac{\nabla_{ad}}{4\pi}\left(\frac{T}{P}\right)\left(\frac{GM_r}{r^4}\right), & \nabla_{rad} > \nabla_{ad} \end{cases}$$

$$\frac{dL_r}{dM_r} = \epsilon(\rho, T, X)$$

Boundary Conditions

At stellar center, $M_r = 0$, $r = L_r = 0$

At stellar surface, $M_r = M$, $\rho = T = 0$

Given $M \Rightarrow L, T_c, P_c$

$$\begin{cases} \frac{dr}{dM} = \frac{1}{4\pi r^2 \rho} \\ \frac{dP}{dM} = -\frac{GM}{4\pi r^2} \\ \frac{dL}{dM} = \epsilon - T\frac{dS}{dT} \\ \frac{dT}{dM} = -\frac{3}{4}\frac{\kappa}{ac}\frac{L}{T^3}\frac{1}{16\pi^2 r^4} \quad \text{(rad.)} \end{cases}$$

$$= \frac{\gamma - 1}{\gamma}\frac{d\ln T}{d\ln P} \quad \text{(conv.)}$$

Given M, μ

→ a stable structure, uniquely determined

Russell - Vogt theorem

⇒ a unique position in H-R diagram for a MS star

⇒ mass-radius & mass-lum. relations

$\kappa \equiv \kappa(\rho, T, \mu)$

$\gamma \equiv \gamma(\rho, T, \mu)$

$$\text{B.C.} \begin{cases} M(r=0) = 0; \ L(r=0) = 0 \\ \rho(r=R) = 0; \ T(r=R) \rightarrow T_{eff} \simeq c \end{cases}$$

∴ Stellar evolution → μ changes

To compute structural changes with appropriate time steps

At a given time, with a given mass

→ set of $(r, T, \rho, \epsilon, L, \mu)$

→ plotted as evolutionary tracks on HRD

e.g. T_{eff}, L

Luminosity

$$\frac{L}{L_\odot} = \frac{L}{L_\odot}(M/M_\odot)$$

$$\frac{L}{L_\odot} \propto \begin{cases} 7^{1.75}(M/M_\odot)^3, & M \gtrsim 7M_\odot \\ (M/M_\odot)^{4.8}, & 0.4M_\odot \lesssim M_\odot \lesssim 7M_\odot \\ 0.4^{2.85}(M/M_\odot)^{1.9}, & M \lesssim 0.4M_\odot \end{cases}$$

Approximately, for $M \gtrsim M_\odot$, $\boxed{L \propto M^{3.5}}$

Main sequence lifetime
($H \to He$)

$$\tau_{MS} \sim 0.1\,\epsilon\,\frac{XM}{L}$$

→ After this fraction stellar evolution becomes important, so star not in stable state

$$\approx 10^{10}\left(\frac{M}{M_\odot}\right)/\left(L/L_\odot\right) \quad [yr]$$

$$\approx 10^{10}(M/M_\odot)^{-2.5} \quad [yr]$$

Note: M-L, strong dependence on mass (index of 3.5) ⇐ strong dep of ϵ on T for $M \gtrsim M_\odot$

Radius

$$\frac{R}{R_\odot} = \frac{R}{R_\odot}(M/M_\odot)$$

$R \sim M^{0.85}$ $\quad M \lesssim M_\odot$
$R \propto M^{0.56}$ $\quad M \gtrsim M_\odot$
} different structure

Temperature

$$\frac{T_c}{T_{\odot,c}} = \frac{T_c}{T_{\odot,c}}(M/M_\odot)$$

$T_{\odot,c} \sim 1.44\times10^7\,K$

- For $M \gtrsim M_\odot$, T_c changes 2-3 x.
- For $M \lesssim M_\odot$, $T_c \uparrow$ as $M \uparrow$

For $T_c \gtrsim 1.4\times10^7\,K$, CNO cycle starts to dominate nuclear reaction process in the core of a star

$T_c < 1.4\times10^7\,K$, PP chain dominates

$$\epsilon_{pp}(\rho, T) \sim \frac{2.4\times10^{4}\rho X^2}{(T/10^9)^{2/3}}\, e^{-3.380/(T/10^9)^{1/3}} \quad [erg\,s^{-1}g^{-1}]$$

$$\epsilon_{CNO}(\rho, T) \sim \frac{4.4\times10^{25}\rho XZ}{(T/10^9)^{2/3}}\, e^{-15.228/(T/10^9)^{1/3}} \quad [erg\,s^{-1}g^{-1}]$$

Evolution Equations

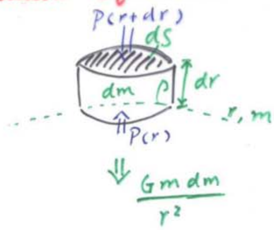

$$dm = \rho\, dr dS = \rho 4\pi r^2\, dr$$

$$\frac{\partial^2 r}{\partial t^2} = \ddot{r}\, dm$$

$$= -\frac{Gmdm}{r^2} + P(r)dS - \underline{P(r+dr)}dS$$

$$P(r) + \frac{\partial P}{\partial r}\cdot dr$$

The equation of motion is

$$\ddot{r} = -\frac{Gm}{r^2} - \frac{1}{\rho}\frac{\partial P}{\partial r} \quad \text{or} \quad \ddot{r} = \frac{Gm}{r^2} - 4\pi r^2 \frac{\partial P}{\partial m}$$

In case of hydrostatic equilibrium, i.e., $\ddot{r} \to 0$

$$\frac{dP}{dr} = -\rho\frac{Gm}{r^2} < 0$$

$X = 0.708$, $Y = 0.272$, $Z = 0.020$

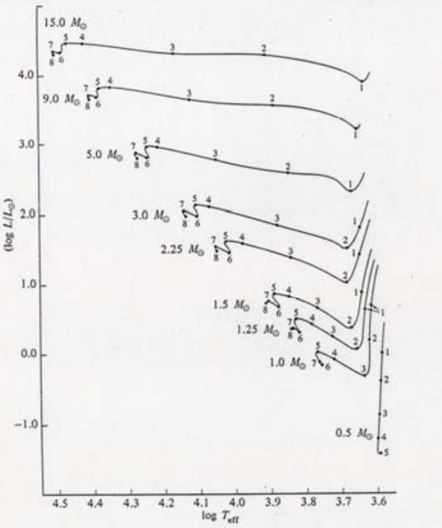

Fig. 7-3A Evolutionary Tracks of Pre-Main-Sequence Stars in the Hertzsprung-Russell Diagram. The mass, in units of the solar mass, is given at the left of each track. The small numbers correspond to the points in Table 7-4A, which give the time measured from the initial model for each mass. The units of T_{eff} are degrees Kelvin. [After I. Iben, Jr., 1965 (321).] ApJ 141, 993

Table 7-4A Time t in Years Measured from the Initial Model for Each Mass. The last point for each mass represents the main sequence.* [From I. Iben, Jr., 1965 (321).]

POINT IN FIG. 7-3A	MASS OF MODEL (UNITS OF THE SOLAR MASS)								
	15	9	5	3	2.25	1.5	1.25	1.0	0.5
	10^4	10^5	10^5	10^6	10^6	10^7	10^7	10^7	10^8
1	0.067	0.014	0.294	0.034	0.079	0.023	0.045	0.012	0.003
2	0.377	0.015	1.069	0.208	0.594	0.236	0.396	0.106	0.018
3	0.935	0.364	2.001	0.763	1.883	0.580	0.880	0.891	0.087
4	2.203	0.699	2.860	1.135	2.505	0.758	1.115	1.821	0.309
5	2.657	0.792	3.137	1.250	2.818	0.862	1.404	2.529	1.550
6	3.984	1.019	3.880	1.465	3.319	1.043	1.755	3.418	—
7	4.585	1.915	4.559	1.741	3.993	1.339	2.796	5.016	—
8	6.170	1.505	5.759	2.514	5.855	1.821	2.954	—	—

* Each entry must be multiplied by 10^n as given at the head of each column.

Table 7-4B The Logarithm of the Time in Seconds, log t, Measured From the Initial Models for Masses 1 $M_\odot$ and 15 $M_\odot$. [From data of I. Iben, Jr., 1965 (321).]

POINT IN FIG. 7-3A	MASS OF MODEL (UNITS OF THE SOLAR MASS)	
	15	1.0
1	10.33	12.57
2	11.07	13.52
3	11.47	14.45
4	11.84	14.76
5	11.92	14.90
6	12.10	15.03
7	12.16	15.20
8	12.29	—

$\log \tau \approx 14.5$

$\log \tau \approx 15.0$

"Introduction to Stellar Atmospheres and Interiors" by Eva Novotny

STELLAR EVOLUTION. I. THE APPROACH TO THE MAIN SEQUENCE*

ICKO IBEN, JR.
California Institute of Technology, Pasadena, California

Received August 18, 1964; revised November 23, 1964

ABSTRACT

The manner in which nuclear reactions replace gravitational contraction as the major source of stellar luminosity is investigated for model stars of population I composition in the mass range $0.5 < M/M_\odot < 15\ 0$. By following in detail the depletion of C^{12} from high initial values down to values corresponding to equilibrium with N^{14} in the C-N cycle, the approach to the main sequence in the Hertzsprung-Russell diagram and the time to reach the main sequence, for stars with $M \geq 1.25\ M_\odot$, are found to differ significantly from data reported previously.

$1\ M_\odot$

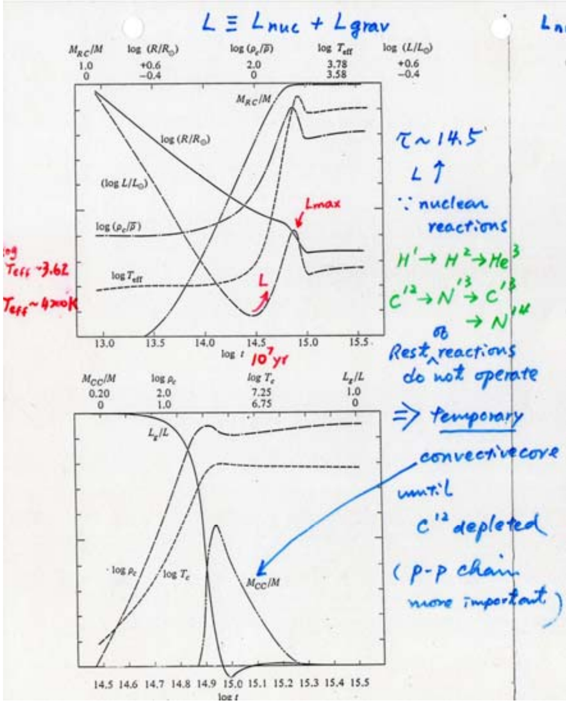

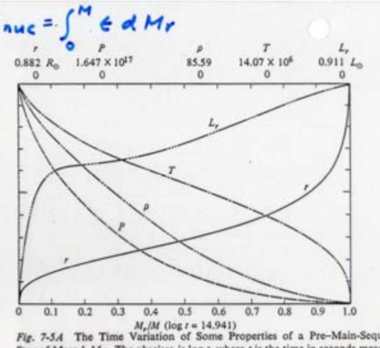

Fig. 7-5A The Time Variation of Some Properties of a Pre–Main-Sequence Star of Mass 1 $M_\odot$. The abscissa is log t, where t is the time in seconds measured from the initial model of the series for this mass. The upper and lower limits of each ordinate are given. The ordinates are: M_{RC}/M, the fraction of the total mass contained in a radiative core; log $(R/R_\odot)$, where $R/R_\odot$ is the total radius relative to that of the Sun ($R_\odot = 6.96 \times 10^{10}$ cm); log $(\rho_c/\bar{\rho})$, where ρ_c is the central density and $\bar{\rho}$ is the mean density; log T_{eff}, where T_{eff} is the effective temperature in degrees Kelvin; and log $(L/L_\odot)$, where $L/L_\odot$ is the luminosity relative to that of the Sun ($L_\odot = 3.86 \times 10^{33}$ erg sec^{-1}). [After I. Iben, Jr., 1965 (321).]

Fig. 7-5B The Time Variation of Some Properties of a Pre–Main-Sequence Star of Mass 1 $M_\odot$. The abscissa is log t, where t is the time in seconds measured from the initial model of the series for this mass. The upper and lower limits of the scale for each curve are given. The ordinates are M_{CC}/M, the fraction of the mass contained in a convective core; log ρ_c, where ρ_c is the central density in gm cm^{-3}; log T_c, where T_c is the central temperature in degrees Kelvin; and L_g/L, the net fraction of the luminosity that is generated by gravitational contraction (but not necessarily the fraction of the *emitted* radiation that is due to gravitational contraction—see text). The value of L_g/L becomes negative near log t = 15.0: zero for this ordinate is on the horizontal axis. [Adapted from I. Iben, Jr., 1965 (321).]

Fig. 7-5C A Model of Mass 1 $M_\odot$ During the Pre–Main-Sequence Phase at Time log t = 14.941. The time is measured in seconds from the initial model of the series for this mass. The abscissa is the fractional mass M_r/M. The upper and lower limits of each ordinate are given. Each upper limit is the maximum value in the model. The ordinates are r, the radius in units of the solar radius ($R_\odot = 6.96 \times 10^{10}$ cm); P, the pressure in dyne cm^{-2}; ρ, the density in gm cm^{-3}; T, the temperature in degrees Kelvin; and L_r, the net luminosity in units of the solar luminosity ($L_\odot = 3.86 \times 10^{33}$ erg sec^{-1}). [Adapted from I. Iben, Jr., 1965 (321).]

Pre-main Sequence Evolution of a 1 $M_\odot$ Star

$\tau < 2 \times 10^{14}$ s (i.e. 7×10^6 yr)

$T_{eff} \sim$ const $\sim$ 4200 K $R \downarrow \Rightarrow L \downarrow$

due to ionization of H & He

a deep convective envelope

$\rho_c/\bar{\rho} \sim$ const   (Hayashi track)

Star completely convective in the first 10^6 yr

L_g/L : energy from gravitational contraction

$\tau \sim 14.5$ (10^7 yr), $L \uparrow \Rightarrow$ nuclear reactions (cont.)

~ 15 $\Rightarrow$ expanding the core

$\rho_c \downarrow$, $T_c \downarrow$

But T_c not high enough

only $^1H \rightarrow {}^2D \rightarrow {}^3He$

$^{12}C \rightarrow {}^{13}N \rightarrow {}^{13}C \rightarrow {}^{14}N$

The rest of PP chains or CNO cycle do **not** operate yet

Note $L_{nuc} + L_g \equiv L$

$\tau \sim 15$, $L_g < 0$ ($\because$ core expansion)

$\epsilon_{nuc} \uparrow \rightarrow \nabla T \uparrow$

$\Rightarrow$ A temporary convective core ($\tau \sim 14.9$)

until ^{12}C is depleted and

PP chains become important

Eventually $\nabla T \downarrow$ at core, convective core $\downarrow$ ($\tau \sim 15.3$)

$\tau \sim 15$, $L \rightarrow L_{max}$

Structure of star adjusts

$\because$ Energy sources from gravitational to nuclear processes

$\Rightarrow$ ^{12}C main sequence ! Point 5

short lasting, depletion rapidly

$\rightarrow$ slight contraction

T_c, ρ_c high enough for pp reactions to be the sole energy source.

For all stars $M \gtrsim M_\odot \Rightarrow$ convective core

^{12}C burning $\longrightarrow$ recedes

For stars $M \gtrsim 1.25\, M_\odot \Rightarrow$ double luminosity maxima and minima

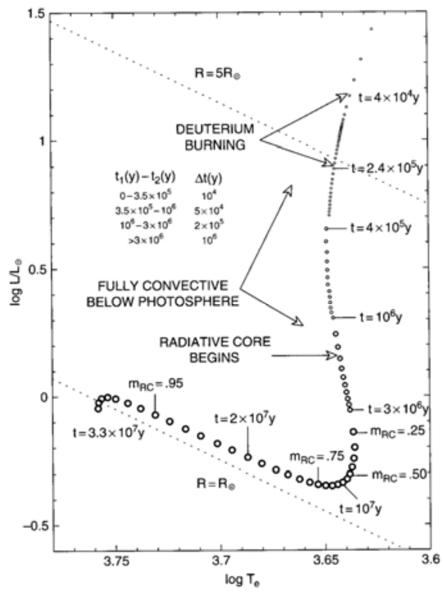

Pre main sequence evolution in the HR diagram of a low mass model ($M = 1M_\odot, Z = 0.01, Y = 0.25$)

Iben 2013

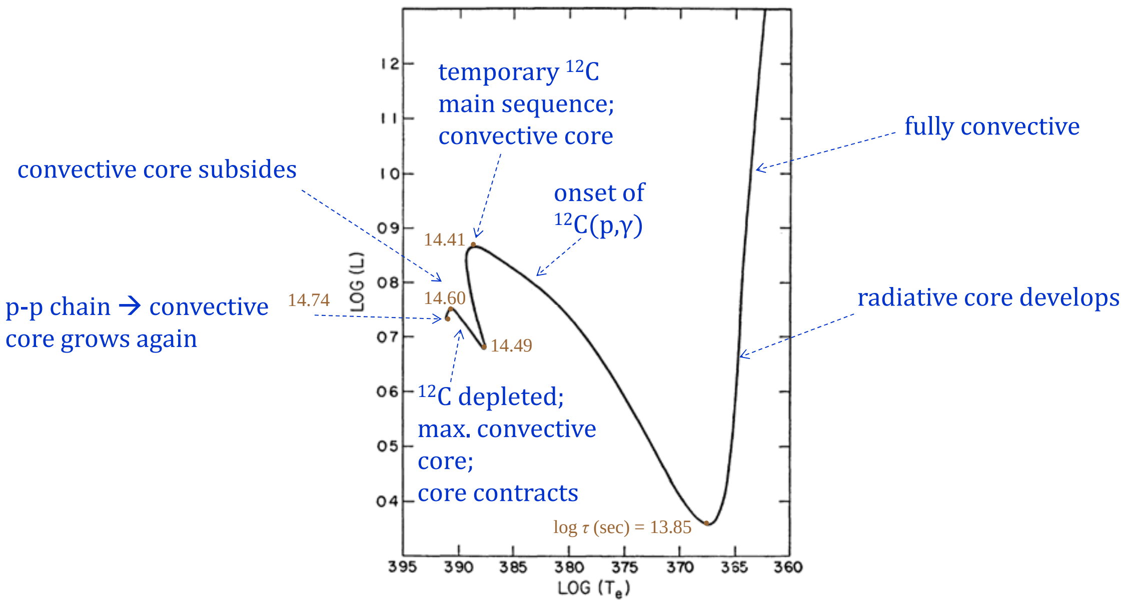

FIG. 6—The path in the Hertzsprung-Russell diagram for $M = 1.5\ M_\odot$. Units of luminosity and surface temperature are the same as in Fig. 1.

For $0.5\,M_\odot$ stars,

ρ_c, T_c not high enough for ^{12}C burning

For $M \lesssim 0.1\,M_\odot$ (dependent on μ)

T_c not high enough for even H burning

$\Rightarrow$ contraction continues

$\rightarrow$ degenerate core

$\Rightarrow$ black dwarfs ... nowadays called brown dwarfs

only the initial, nearly vertical descent

$\because$ T_c, ρ_c never high enough to ignite ^{12}C

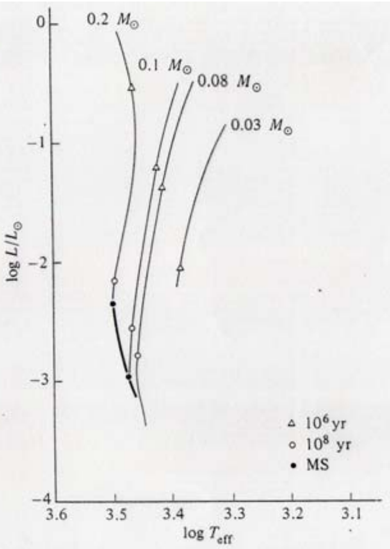

Fig. 7-3B Evolutionary Tracks of Pre–Main-Sequence Stars of Low Mass in the Hertzsprung–Russell Diagram. The masses, and the ages at two points on each track, are indicated. The heavy curve (*MS*) is the hydrogen-burning main sequence. The convective parameter is assumed to have the value $l/H = 1.0$. [Adapted from A. S. Grossman and H. C. Graboske, Jr., 1971 (400).]

Parameters at the stellar cores for non-rotating single MS stars

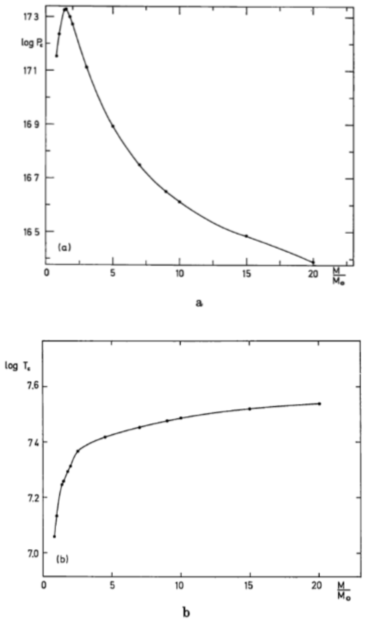

Figs. 3a and 3b. For non-rotating stars, the central pressure and central temperature variation with mass along the main-sequence

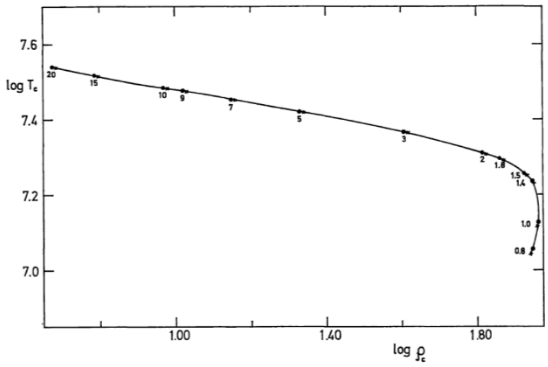

Fig. 4. The central temperature versus the central density for main-sequence stars. The curve is drawn through the data referring to non-rotating stars (dots). The crosses refer to critically, uniformly rotating stars. The Arabic numeral refers to the mass of the model

Sackman (1970) A&A, **8**, 76

Effect of Stellar Rotation

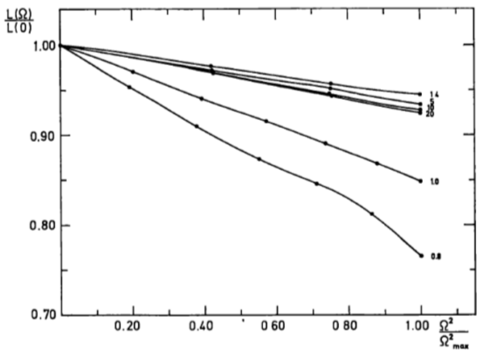

Fig. 1. The decrease of the luminosity with increasing rotation measured by Ω^2/Ω^2_{max}, where Ω refers to the angular velocity of rotation and the subscript max to the critical case. The Arabic numeral refers to the mass of each sequence in solar units

$\frac{\Omega}{\Omega_{crit}} \nearrow \Rightarrow L \searrow$

More so for lower-mass stars

Rotation effectively lowers the stellar mass.

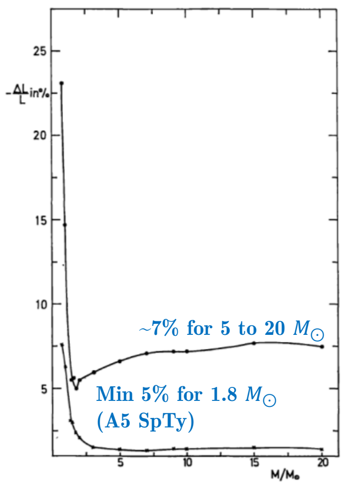

Fig. 5. The maximum change in the luminosity of a critically rotating star from that of a non-rotating star of the same mass, expressed in percent, against the mass of the main-sequence model. The dots refer to the actual results of the Stellar Interior models, while the crosses refer to the approximations made for Eq. (12)

Sackman (1970) ApJ, **8**, 76

Rotation → star cooler and fainter

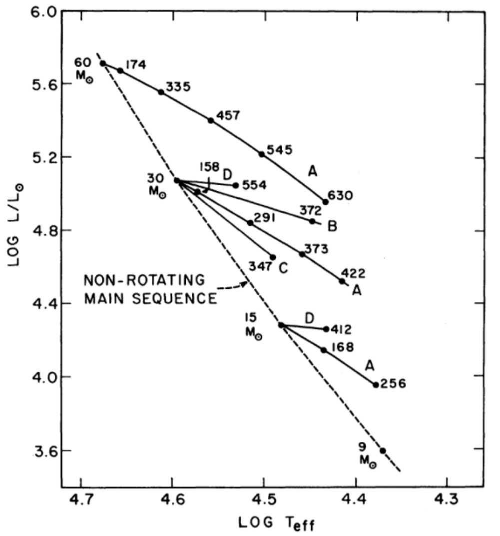

Fig. 2.—Theoretical H-R diagram showing model sequences of increasing angular momentum (*solid curves*). Numbers on curves give calculated velocities at the equator in km sec^{-1}. The distribution of angular momentum for each sequence is indicated by the letter A, B, C, or D.

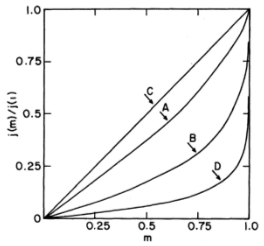

Fig. 1.—Angular momentum per unit mass, as a function of mass fraction interior to a given cylinder about the axis of rotation, for three assumed laws of differential rotation (Cases A, B, and C) and for a uniformly rotating model (Case D) of 30 $\mathfrak{M}_\odot$, log J = 52.73.

D: solid body rotation

Rotation law:
angular momentum distribution $j(m_\varpi)$ as a function of, m_ϖ, the mass fraction interior to the cylinder of radius ϖ about the rotation axis.

Bodenheimer (1971) ApJ, **167**, 153

Rotation → line broadening

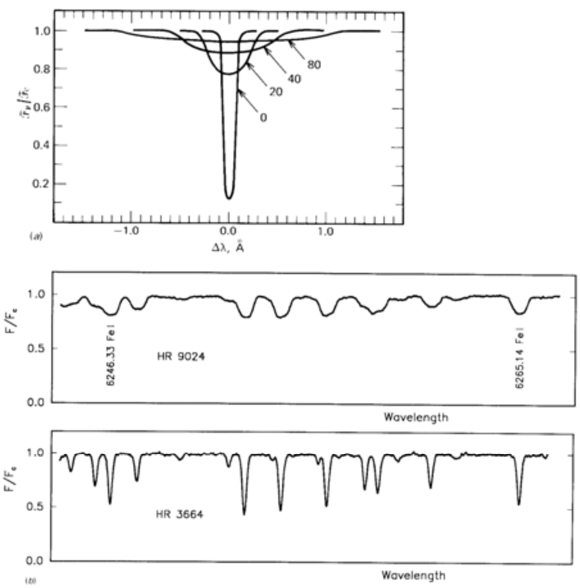

Fig. 17.7. (*a*) Computed profiles illustrate the broadening effect of rotation. The profiles are labeled with $v \sin i$. the wavelength is 4243 Å, and the line has an equivalent width of 100 mÅ. (*b*) These two early-G giants illustrate the Doppler broadening of the line profiles by rotation.

Gray p. 376

Rotation vs Spectral Type

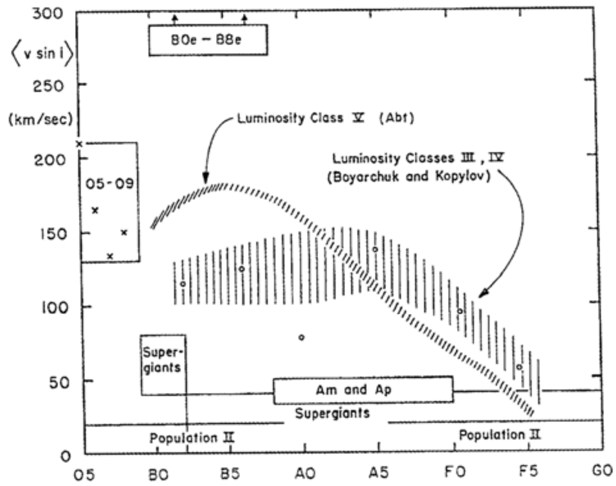

Fig. 3. Projected equatorial velocities, averaged over all possible inclinations, as a function of spectral type. On the main sequence (luminosity class V), early-type stars have rotational velocities that reach and even exceed 200 km/s; these velocities drop to a few km/s for late-type stars, such as the Sun (type G2) (Slettebak [20]; courtesy Gordon & Breach)

15 $M_\odot$

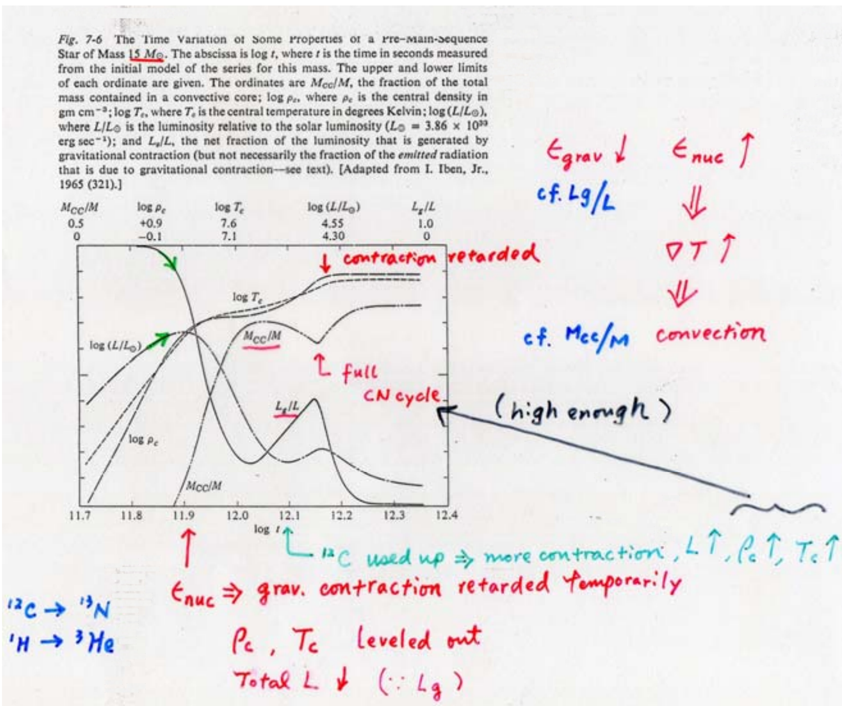

Fig. 7-6 The Time Variation of Some Properties of a Pre-Main-Sequence Star of Mass 15 $M_\odot$. The abscissa is log t, where t is the time in seconds measured from the initial model of the series for this mass. The upper and lower limits of each ordinate are given. The ordinates are M_{CC}/M, the fraction of the total mass contained in a convective core; log ρ_c, where ρ_c is the central density in gm cm^{-3}; log T_c, where T_c is the central temperature in degrees Kelvin; log $(L/L_\odot)$, where $L/L_\odot$ is the luminosity relative to the solar luminosity ($L_\odot = 3.86 \times 10^{33}$ erg sec^{-1}); and L_g/L, the net fraction of the luminosity that is generated by gravitational contraction (but not necessarily the fraction of the *emitted* radiation that is due to gravitational contraction—see text). [Adapted from I. Iben, Jr., 1965 (321).]

1997AJ....113.1733H

Stellar population and Star formation history

⟨Av⟩ ~ 2.15

Herbig & Turndrup (1986)

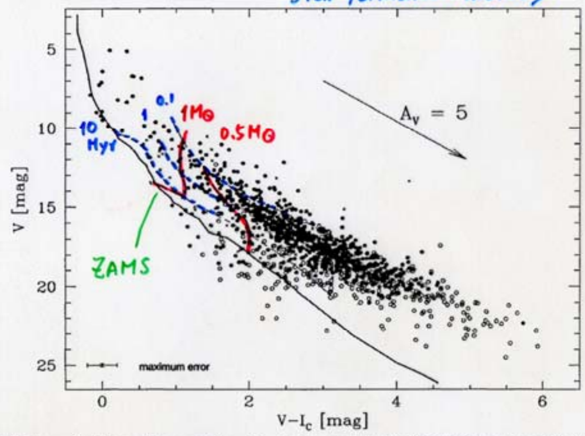

FIG. 7. *Color-magnitude diagram for all stars with measured V- and I-band photometry.* Errors for the new photometry are smaller than 0.05 mag in V and 0.1 mag in $V-I_C$ in 90% of the cases and are restricted in all cases to 0.1 mag in V and 0.2 mag in $V-I_C$, corresponding to the error bar shown. Also shown is the reddening vector corresponding to 5 magnitudes of visual extinction and the zero-age main sequence over the range O5–M7, as well as the 0.1, 1, and 10 Myr isochrones and the 0.5 and 1 $M_\odot$ evolutionary tracks from the calculations of D'Antona & Mazzitelli (1994) translated into this color-magnitude plane. Filled circles indicate proper motion cluster members plus all sources which have been identified as being externally ionized; open circles indicate that no proper motion information is available; crosses indicate proper motion nonmembers.

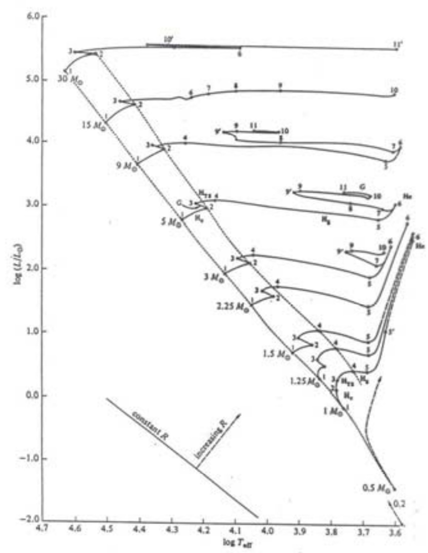

H_c : H core burning

H_{TS} : H thick shell

T_s : H thin shell

Table 7-7 Evolutionary Times. The times, expressed in years, refer tervals between the points in Fig. 7-25.* [Adapted from I. Iben, Jr., 1967 (327).]

MASS ($M_\odot$) \ INTERVAL	1–2	2–3	3–4	4–5	5–6
30	4.80 (6)	8.64 (4)	←	~1.0 (4)	→
15	1.010 (7)	2.270 (5)	←	7.55 (4)	→
9	2.144 (7)	6.053 (5)	9.113 (4)	1.477 (5)	6.552 (4)
5	6.547 (7)	2.173 (6)	1.372 (6)	7.532 (5)	4.857 (5)
3	2.212 (8)	1.042 (7)	1.033 (7)	4.505 (6)	4.238 (6)
2.25	4.802 (8)	1.647 (7)	3.696 (7)	1.310 (7)	3.829 (7)
1.5	1.553 (9)	8.10 (7)	3.490 (8)	1.049 (8)	≥2 (8)
1.25	2.803 (9)	1.824 (8)	1.045 (9)	1.463 (8)	≥4 (8)
1.0	7 (9)	2 (9)	1.20 (9)	1.57 (8)	≥1 (9)

MASS ($M_\odot$) \ INTERVAL	6–7	7–8	8–9	9–10(?)	10(?)–11(?)
30	←	53.1 (4)	→		1.3 (4)
15	7.17 (5)	6.20 (5)	1.9 (5)	3.5 (4)	
9	4.90 (5)	9.50 (4)	3.28 (6)	1.55 (5)	2.86 (4)
5	6.05 (6)	1.02 (6)	9.00 (6)	9.30 (5)	7.69 (4)
3	2.51 (7)	4.08 (7)		6.00 (6)	

* A number in parentheses is the power of 10 by which an entry is to be multiplied.

Fig. 7-25 Evolutionary Tracks in the Hertzsprung–Russell Diagram. The mass of each star is given at the left of the track. The composition is $X = 0.708$, $Y = 0.272$, and $Z = 0.020$ for all masses except 30 $M_\odot$, for which the composition is $X = 0.70$, $Y = 0.27$, $Z = 0.03$. *Dashed portions* of the curves are estimates. The *letters* along the tracks for 1 $M_\odot$ and 5 $M_\odot$ have the following significance: H_c = hydrogen-burning near the center; G = gravitational contraction of the entire star; H_{TS} = hydrogen-burning in a thick shell; H_S = hydrogen-burning in a thin shell; He = helium-burning near the center plus hydrogen-burning in a thin shell. The times required to reach the encircled points are given in Table 7-7.

The *dotted lines* indicate the boundaries of the main sequence. The *line* (*lower left*) shows the slope of a path along which the radius remains constant. The track for 15 $M_\odot$ does not turn back as do the other tracks because the semi-convective zone was treated as fully convective [see R. Stothers and C.-W. Chin, 1968 (377)]. [Adapted from I. Iben, Jr., 1967 (327). The track for 30 $M_\odot$ is given by R. Stothers, 1966 (333).]

Evolution on the Main Sequence

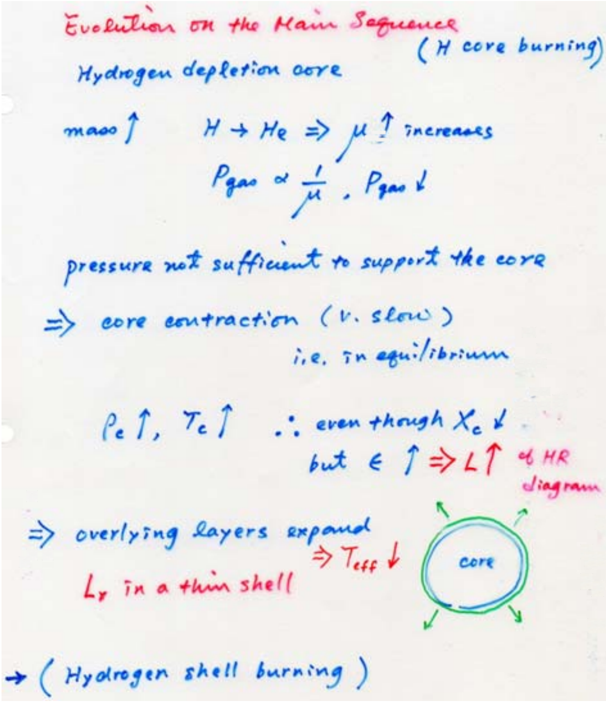

1-2 main sequence
2-3 overall contraction
3-4 H thick shell burning
5-6 H thin shell burning
6-7 red giant
7-10 core He burning
8-9 envelope contraction

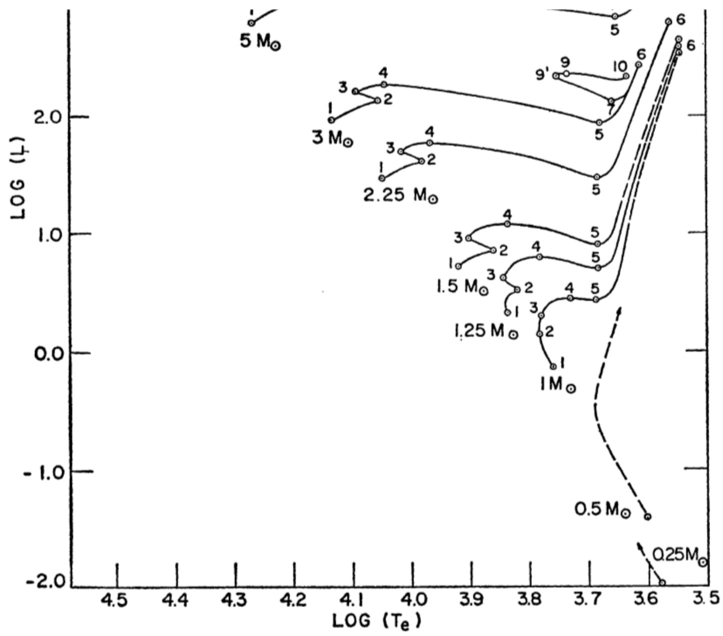

$\frac{dL_r}{dM_r} = \epsilon$ v. high near center

↓ slope

H depletion core

$X \simeq 0,\ L_r \simeq 0,\ \nabla T \simeq 0$

$\Rightarrow \epsilon_{nuc}$ in a thin shell

298 Stellar Interiors

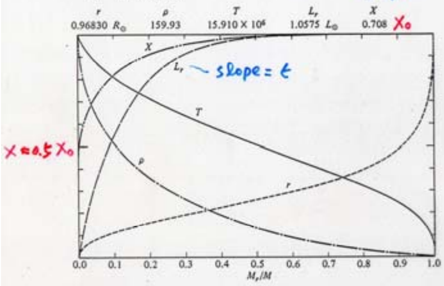

Fig. 7-10A A Model of Mass 1 $M_\odot$ during the Main-Sequence Phase at Time $t = 4.26990 \times 10^9$ Years. Radius r, density ρ, temperature T, net luminosity L_r, and hydrogen abundance X are shown as functions of fractional mass M_r/M. The lower limit of the ordinate is zero for all variables. The upper limits, given in the figure, are the total radius R (units of $R_\odot = 6.96 \times 10^{10}$ cm), central density ρ_c (gm cm^{-3}), central temperature T_c in degrees Kelvin, total luminosity L (units of $L_\odot = 3.86 \times 10^{33}$ erg sec^{-1}), and initial hydrogen abundance $X = 0.708$. The central pressure (not shown) is 2.5186×10^{17} dyne cm^{-2}. The time t is measured from the initial model calculated for the pre-main-sequence phase (see Section 2). [Adapted from I. Iben, Jr., 1967 (326).]

Zero-age Main Sequence (ZAMS)
≡ homogeneous chemical composition

Termination of MS
≡ end of H burning at core

299 Stellar Evolution

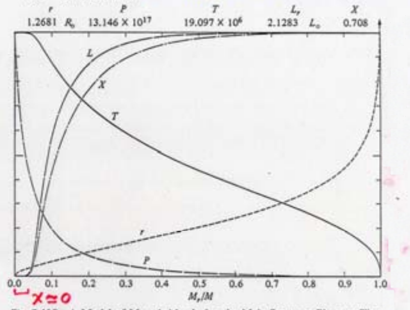

Fig. 7-10B A Model of Mass 1 $M_\odot$ during the Main-Sequence Phase at Time $t = 9.20150 \times 10^9$ Years. Radius r, pressure P, temperature T, net luminosity L_r, and hydrogen abundance X are shown as functions of fractional mass M_r/M. The lower limit of the ordinate is zero for all variables. The upper limits, given in the figure, are 1.2681 $R_\odot$ (with $R_\odot = 6.96 \times 10^{10}$ cm; however, the total radius is 1.3526 $R_\odot$), central pressure P_c (dyne cm^{-2}), central temperature T_c in degrees Kelvin, total luminosity L (units of $L_\odot = 3.86 \times 10^{33}$ erg sec^{-1}), and initial hydrogen abundance $X = 0.708$. The central density (not shown) is 1026.0 gm cm^{-3}. The time t is measured from the initial model calculated for the pre-main-sequence phase (see Section 2). [Adapted from I. Iben, Jr., 1967 (326).]

As τ goes on, $M_{core}^{H=0}$ ↑, until $M_c \sim 0.1\ M_\odot$

Schönberg-Chandrasekhar limit (1942) ApJ 96, 16

maximum fraction of total mass maintainable within an isothermal core

1 $M_\odot$ Stars on the Main Sequence

$4H \rightarrow He$ $\quad n\downarrow \rightarrow P\downarrow \rightarrow$ core contracts (slowly)

$q_{pp} \sim \rho X^2 T_6^4$

H depletion $X\downarrow$ but $T\uparrow$, $\rho\uparrow$

$\therefore q\uparrow \Rightarrow L\uparrow$

(Faint distant sun dilemma)

→ envelope $R\uparrow$

H depleted core $L_r = 0$, but ϵ_{nuc} in a thick shell around the core

$$L_{TS} > L_{core\,(MS)}$$

$$\Rightarrow L \uparrow \rightarrow R \uparrow \Rightarrow T_{eff} \downarrow$$

Point 4 ≡ End of M.S

Star → subgiant branch

until M_{sc} is reached ($\sim$8-10%)

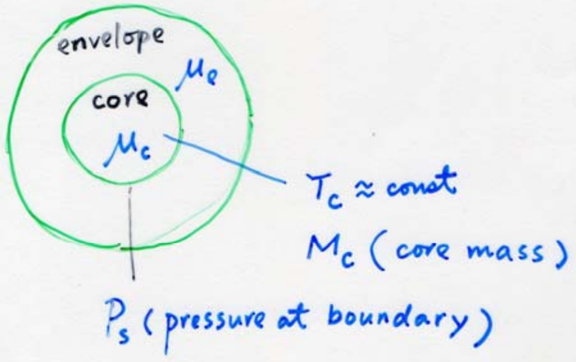

THE ASTROPHYSICAL JOURNAL

AN INTERNATIONAL REVIEW OF SPECTROSCOPY AND ASTRONOMICAL PHYSICS

VOLUME 96 SEPTEMBER 1942 NUMBER 2

ON THE EVOLUTION OF THE MAIN-SEQUENCE STARS

M. Schönberg[1] and S. Chandrasekhar

ABSTRACT

The evolution of the stars on the main sequence consequent to the gradual burning of the hydrogen in the central regions is examined. It is shown that, as a result of the decrease in the hydrogen content in these regions, the convective core (normally present in a star) eventually gives place to an isothermal core. It is further shown that there is an upper limit (~ 10 per cent) to the fraction of the total mass of hydrogen which can thus be exhausted. Some further remarks on what is to be expected beyond this point are also made.

$$\frac{M_c}{M} \approx 0.37 \left(\frac{\mu_e}{\mu_c} \right)^2 \quad (\sim 10\text{-}15\% \text{ in reality})$$

Take ionized H in env ($\mu = 0.61$); pure He in core $\mu = 1.34$

$M_c \sim 8\text{-}9\%\, M$ $\mu_c \sim 2\,\mu_e$

Beech 1988

(Point 4, 5) Shortly after the MS

- ϵ_{nuc} in a thin shell
- L_r ↑↑ between 13% - 20%
- core experiences gravitational contraction $L_g > 0$
  $\Rightarrow \nabla T$
- $\rho_c \to 1.5 \times 10^4$ g cm^{-3}, P_{deg} important ($= 0.46\, P_{total}$)
- convection beyond 63% M → mixing → $X \approx$ const

(Point 5′) $P_{deg} = 76\% \; P_{total}$

$T_{shell} \uparrow\uparrow$ $\quad \epsilon_{CN} > \epsilon_{pp} \Rightarrow R\uparrow\uparrow, \; T_{eff} \downarrow\downarrow$

$\kappa \uparrow$ in envelope → convection for outer

71 2% 71% M

X ≃ const ~~for outer~~ 29% M beyond

∇T in core ← grav. contraction

$\rho_c = 1.5 \times 10^4 \; g\,cm^{-3} \Rightarrow P_{deg} = 46\%$ of P_{total}

ϵ in a shell

So $M_c > M_{sc}$ OK

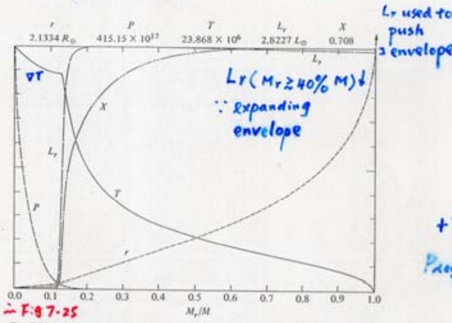

H-5 ≈ Fig 7-25

Fig. 7-26A A Model of Mass 1 $M_\odot$ Shortly after Leaving the Main Sequence, at $t = 10.3059 \times 10^9$ Years. Radius r, pressure P, temperature T, net luminosity L_r, and hydrogen abundance X are shown as functions of fractional mass M_r/M. The lower limit of the ordinate is zero for all variables. The upper limits, given in the figure, are 2.1334 $R_\odot$ (with $R_\odot = 6.96 \times 10^{10}$ cm; however, the total radius is 2.2179 $R_\odot$), central pressure P_c (dyne cm^{-2}), central temperature T_c (°K), total luminosity L (units of $L_\odot = 3.86 \times 10^{33}$ erg sec^{-1}), and initial hydrogen abundance $X = 0.708$. The central density (not shown) is 15,214 gm cm^{-3}. The time is measured from the initial model calculated for the pre-main-sequence phase (see Section 2). [Adapted from I. Iben, Jr., 1967 (326).]

X ≃ const > 63% M ∵ convection (mixing)

$\rho_c \sim 10^5 \; g\,cm^{-3}$ $\quad \frac{P_{deg}}{P_{tot}} \sim 76\%$

$T_s \uparrow\uparrow \Rightarrow \epsilon_{CN} > \epsilon_{pp}$

X(M > 30%) ≃ const ∵ convection

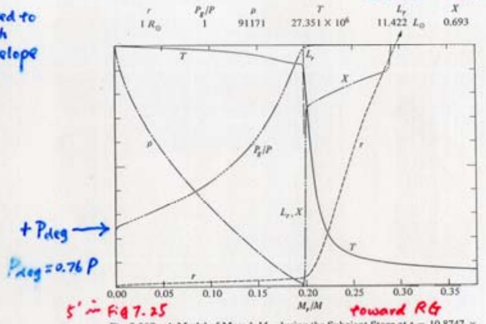

5′ ≈ Fig 7.25 $\quad$ toward RG

Fig. 7-26B A Model of Mass 1 $M_\odot$ during the Subgiant Stage at $t = 10.8747 \times 10^9$ Years. Radius r, ratio P_g/P of gas pressure computed from the perfect gas law to the actual pressure with degeneracy included, temperature T, net luminosity L_r, and hydrogen abundance X are shown as functions of fractional mass M_r/M in the range 0 to 0.38. The distribution of L_r is a step function rising from zero to maximum scale with the initial rise in X. The lower limit of the ordinate is zero for all variables. The upper limits, given in the figure, are 1 $R_\odot$ (with $R_\odot = 6.96 \times 10^{10}$ cm; however, the total radius is 6.1784 $R_\odot$), unity for the ratio of pressures, central density ρ_c (gm cm^{-3}), central temperature T_c (°K), total luminosity L (units of $L_\odot = 3.86 \times 10^{33}$ erg sec^{-1}), and hydrogen abundance $X = 0.693$. The central pressure (not shown) is 6552.2 dyne cm^{-2}. The time is measured from the initial model calculated for the pre-main-sequence phase (see Section 2). [Adapted from I. Iben, Jr., 1967 (326).]

Envelope expands and cools

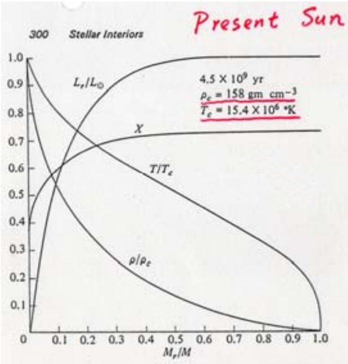

Fig. 7-11A A Model Solar Interior. Density relative to the central density ρ/ρ_c, temperature relative to central temperature T/T_c, net luminosity relative to total luminosity $L_r/L_\odot$, and hydrogen abundance X are shown as functions of fractional mass M_r/M. The chemical composition is $X = 0.730$, $Y = 0.245$, and $Z = 0.025$. The age is 4.5×10^9 years. [After S. Torres-Peimbert, E. Simpson, and R. K. Ulrich, 1969 (329).]

$X_c = 0.376$

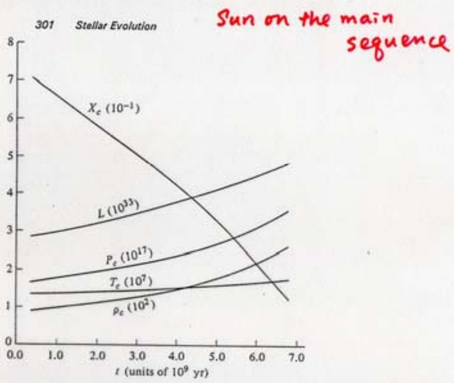

Fig. 7-11B The Evolution of the Sun during 7 Billion Years. Total luminosity L and central values of pressure P_c, temperature T_c, density ρ_c, and hydrogen abundance X_c are shown as functions of time t, which is measured from the initial (homogeneous) state for which the composition is $X = 0.730$, $Y = 0.245$, and $Z = 0.025$. The power of ten by which each value must be multiplied is indicated in parentheses. The values of P_c, ρ_c, and L are expressed in cgs units, and T_c is expressed in degrees Kelvin. [After S. Torres-Peimbert, E. Simpson, and R. K. Ulrich, 1969 (329).]

$P_{deg} \sim 0.017 P_{total}$ at ZAMS

0.075 9.2×10^9 yr

(Fig 7-10B)

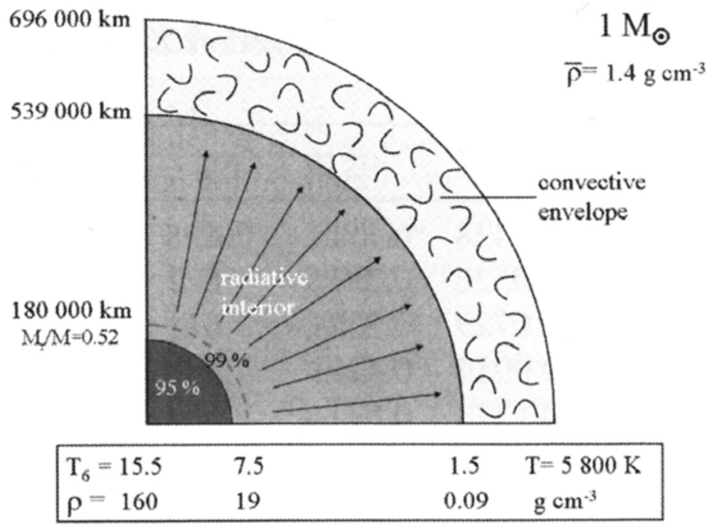

Figure 3.2. The present structure of the Sun. The physical parameters are indicated in the figure. The temperature T_6 is in million K. *From Maeder (2009).*

Lequeux 2013

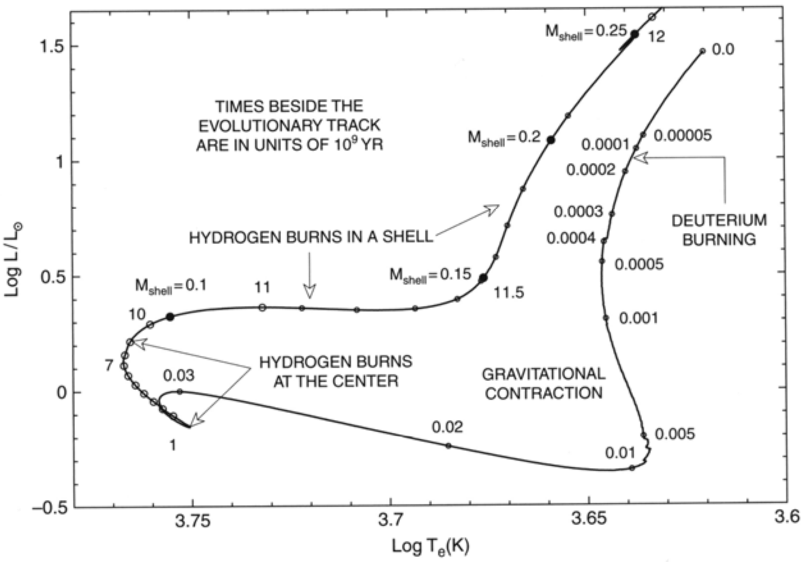

Evolutionary track of a 1M$_\odot$ model ($Z = 0.015$, $Y = 0.275$) during gravitational contraction and central and shell hydrogen-burning phases

Iben 2013

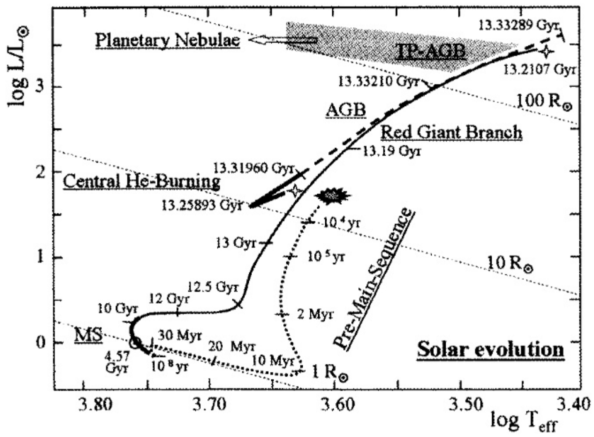

Figure 3.1. The evolution of the Sun. The evolution track of a solar-mass star is shown in the HR diagram from its formation to its death as a planetary nebula. Time is indicated at different steps along the track. The two 4-branch stars correspond to the helium flash and to the subsequent rapid rearrangement of the structure of the star. *From Maeder (2009), data from Corinne Charbonnel.*

Lequeux 2013

Effect of Chemical Composition

As X ↑ & Z ↑

⇒ MS shifts upwards

Given a mass, shifted to the right and downwards

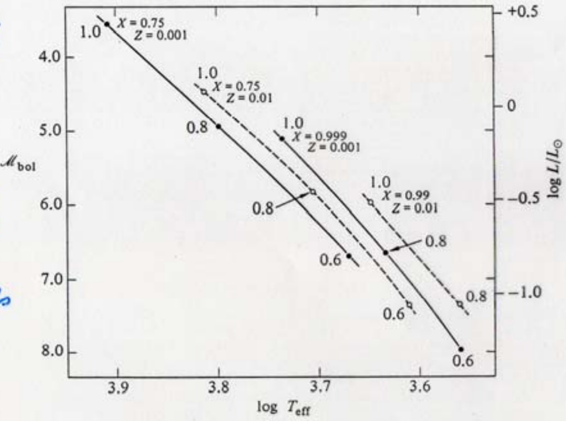

Fig. 7-15A The Effect of Chemical Composition on the Main Sequence in the Hertzsprung–Russell Diagram. Each curve is calculated for a different chemical composition. The masses 0.6 $M_\odot$, 0.8 $M_\odot$, and 1.0 $M_\odot$ are indicated. [From P. Demarque, 1960 (369).]

For Pop I $\left(\begin{array}{c} 0.57 \lesssim X \lesssim 0.77 \\ 0.01 \lesssim Z \lesssim 0.03 \end{array} \right)$ $\Delta m_{bol} \sim 0.8$ mag for 1 $M_\odot$

Pop II similar range in Δm_{bol}

Main Sequence phase = core H burning

Evidence of thermonuclear reactions at a star's center, i.e., stellar evolution

- (solar) neutrinos
- heavy elements in evolved stars (isotope ratios ≠ YSOs)

  'dredge-up' ← convective zone to bring processed materials to surface
- Stars "disappear", e.g., supernovae

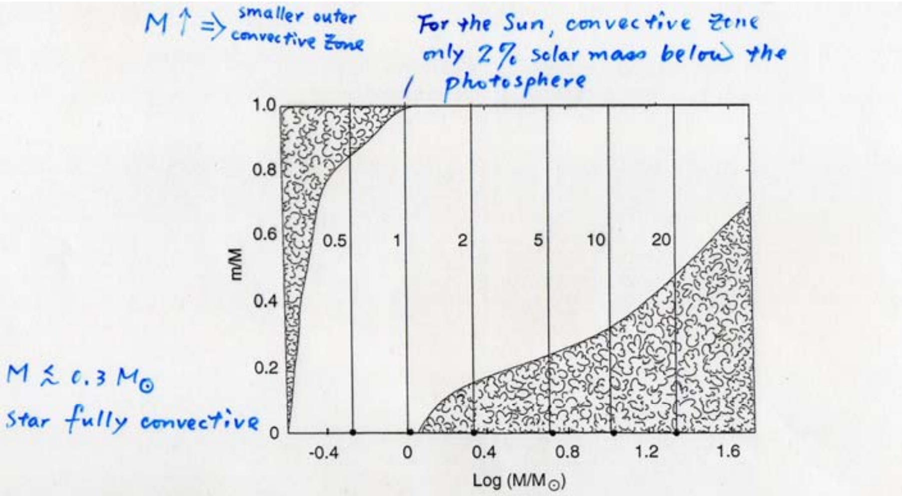

Figure 8.4 The extent of convective zones (shaded areas) in main-sequence star models as a function of the stellar mass [adapted from R. Kippenhahn & A. Weigert (1990), *Stellar Structure and Evolution*, Springer-Verlag].

Subdwarfs: The Pop II Main Sequence

- Luminosity class VI
- 1.5 to 2 mag fainter than a Pop I MS stars o the same spectral type
- Low metallicity → low opacity → (UV excess) → low radiation pressure, so smaller, hotter for the same stellar mass

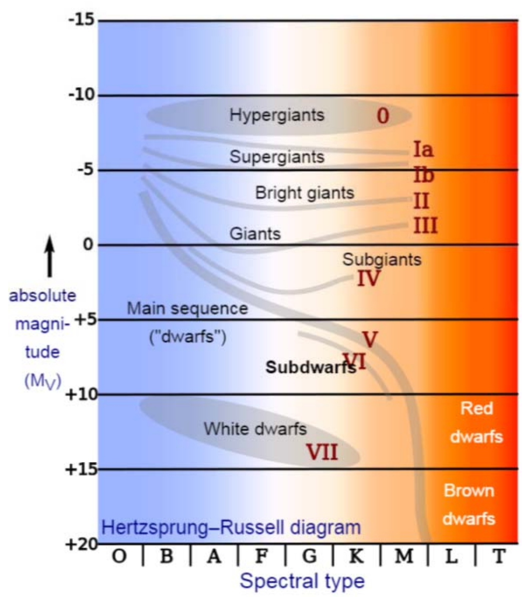

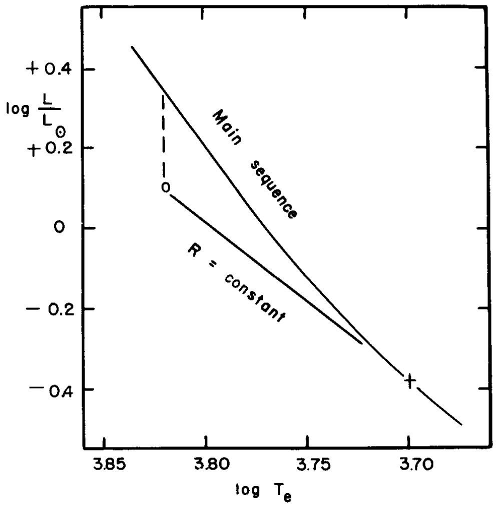

Fig. 17.1. Relation of subdwarfs to the main-sequence in the Hertzsprung-Russell diagram.

Schwarzschild